Molecular Imaging of Conscious, Unrestrained Mice with AwakeSPECT

Justin S. Baba[1], Christopher J. Endres[2], Catherine A. Foss[2], Sridhar Nimmagadda[2], Hyeyun Jung[2], James S. Goddard[1], Seungjoon Lee[3], John McKisson[3], Mark F. Smith[4], Alexander V. Stolin[5], Andrew G. Weisenberger[3], and Martin G. Pomper[2]

[1]Oak Ridge National Laboratory, Oak Ridge, Tennessee; [2]Russell H. Morgan Department of Radiology and Radiological Science, Johns Hopkins Medical Institutions, Baltimore, Maryland; [3]Thomas Jefferson National Accelerator Facility, Newport News, Virginia; [4]Department of Diagnostic Radiology and Nuclear Medicine, University of Maryland School of Medicine, Baltimore, Maryland; and [5]Department of Radiology, West Virginia University, Morgantown, West Virginia

We have developed a SPECT imaging system, AwakeSPECT, to enable molecular brain imaging of untrained mice that are conscious, unanesthetized, and unrestrained. We accomplished this with head tracking and motion correction techniques. **Methods:** The capability of the system for motion-corrected imaging was demonstrated with a ^{99m}Tc-pertechnetate phantom, ^{99m}Tc-methylene diphosphonate bone imaging, and measurement of the binding potential of the dopamine transporter radioligand ^{123}I-ioflupane in mouse brain in the awake and anesthetized (isoflurane) states. Stress induced by imaging in the awake state was assessed through measurement of plasma corticosterone levels. **Results:** AwakeSPECT provided high-resolution bone images reminiscent of those obtained from CT. The binding potential of ^{123}I-ioflupane in the awake state was on the order of 50% of that obtained with the animal under anesthesia, consistent with previous studies in nonhuman primates. Levels of stress induced were on the order of those seen in other behavioral tasks and imaging studies of awake animals. **Conclusion:** These results demonstrate the feasibility of SPECT molecular brain imaging of mice in the conscious, unrestrained state and demonstrate the effects of isoflurane anesthesia on radiotracer uptake.

Key Words: awake; mouse; SPECT; anesthesia; ioflupane

Preclinical molecular imaging of the brain can be applied to studying aspects of brain chemistry, development of mechanism-based imaging agents, and drug development (1–4). Such studies are accomplished with high-resolution optical methods that require surgical exposure of the cortex or lower-resolution nonoptical molecular imaging techniques (5,6). Examples of the latter include MR imaging, PET, SPECT, and photoacoustic tomography (1,7–9). Although intravital microscopy provides a gold standard for live brain imaging, it is laborious and requires considerable expertise. Compared with intravital microscopy, noninvasive methods such as PET and SPECT are less operator dependent; however, anesthesia or physical restraint is required during image acquisition to prevent animal motion and blurring of the images. Current technologies and approaches for imaging animals or organs when motion is regular or periodic, such as cardiac or respiratory motion, are ineffective for imaging in the presence of unpredictable voluntary head motion; therefore, physical or chemical restraint is required. Such restraint may perturb aspects of normal physiology, such as blood flow and brain metabolism, and lead to inaccurate results.

The desire to acquire images in the conscious state has promoted a trend toward imaging animals in the awake state. However, in most cases, imaging of awake animals has meant that the animals were conscious during the injection and uptake of a radiotracer and then anesthetized or sacrificed immediately before imaging (10). In such studies, dynamic imaging in a single animal is not possible. Occupancy or pharmacologic challenge studies cannot be performed without the sacrifice of numerous animals at a variety of time points after injection.

Chemical restraint to facilitate brain imaging in small-animal models, although effective in minimizing motion blur, introduces other complications. Anesthesia can have profound effects on cerebral blood flow, rates of oxygen metabolism and glucose utilization, receptor expression, and perhaps even receptor occupancy, suggesting that results obtained under anesthesia may not accurately report the variable of interest (7,9,11,12). The need to image awake animals without anesthesia has led to the use of methods that attempt to avoid or minimize physical restraint (8,11,13–15), with the underlying assumption that head restraint will have a negligible impact on brain physiology. However, physical restraint may trigger stress and anxiety, which can alter cerebral blood flow and glucose consumption (14,16,17).

We recently developed a system, AwakeSPECT, to enable imaging of conscious, untrained, unanesthetized,

freely moving mice within a near-infrared (NIR)–transparent burrow (Fig. 1) (*18*). AwakeSPECT tracks NIR reflective markers on the mouse's head to measure motion as the SPECT scan is being acquired and then uses this information to compensate for motion during image reconstruction. Here we present the results obtained from 4 sets of studies conducted with AwakeSPECT; the results demonstrated the capabilities of the system and then were used to assess the effects of anesthesia on a clinically relevant brain imaging agent.

The first set of studies tested the capability of the system to perform motion-corrected, 3-dimensional imaging of a high-resolution moving phantom filled with ^{99m}Tc-pertechnetate. The second set demonstrated the capability of AwakeSPECT to image a moving, awake mouse after administration of the bone imaging agent ^{99m}Tc-methylene diphosphonate (^{99m}Tc-MDP). A nonimaging study set investigated the level of stress experienced by mice imaged with AwakeSPECT by measuring serum corticosterone levels. Last, a set of studies with awake mice was conducted to investigate the effects of anesthesia on the uptake of ^{123}I-ioflupane (DaTSCAN; GE Healthcare) (*19*). ^{123}I-Ioflupane is a radioiodinated cocaine analog with a high affinity for the dopamine transporter. One indication for ^{123}I-ioflupane is to help differentiate dementia with Lewy bodies from Alzheimer disease (*20*).

MATERIALS AND METHODS

Hardware

AwakeSPECT (Fig. 1) tracks head position (3 translational and 3 rotational degrees of freedom) as a function of time. Together with information on the rotating γ-camera position and with time-stamped, list-mode data for detected photons, motion-corrected image reconstruction is performed with an iterative maximum-likelihood expectation maximization algorithm. The development and testing of the AwakeSPECT system are described elsewhere (*18,22*).

For SPECT studies, the pinhole diameter was 1.5 mm, the focal length (distance from pinhole to detector) was 111.1 mm, and the distance from the pinhole to the axis of rotation (AOR) was 49.3 mm, for a magnification of 2.25. Image reconstruction was accomplished by use of the maximum-likelihood expectation maximization algorithm with 40 iterations, a 0.5-mm voxel size, and postfiltering with a 3-dimensional, 0.6-mm full width at half maximum gaussian function. Decay correction was applied.

Phantom Study

The capability of the system to perform motion-compensated SPECT imaging was initially tested by use of Ultra-Micro Phantoms (Data Spectrum Corp.) with hot-rod and Defrise inserts and without an insert and uniform activity. The phantom cylinder has an inside diameter of 2.8 cm and an inside height of 2.8 cm. The hot-rod insert is 1 cm high and has 6 sectors of hot rods with diameters of 0.75, 1.0, 1.35, 1.7, 2.0, and 2.4 mm and a center-to-center hole spacing of twice the hole diameter. The Defrise insert has 8 solid disks, each with a thickness of 1.62 mm, and a gap of 1.62 mm between the disks. There is a central cold rod supporting the disks. Three retroreflectors were mounted on the outside of the phantom to allow its position to be tracked.

The phantom was filled with ^{99m}Tc-pertechnetate solution before imaging experiments: 284 MBq (7.67 mCi) for the hot-rod insert, 89 MBq (2.41 mCi) for the Defrise insert, and 93 MBq (2.52 mCi) for the uniform phantom. Each phantom was imaged twice, once without motion and once with random motion produced by hand. γ-Ray data were obtained at 60 equally spaced γ-camera stops over 360° with a 6° increment and a 30-s acquisition at each γ-camera position. The energy window was 125–155 keV. Three sets of images were formed: static phantom, moving phantom with no motion compensation, and moving phantom with motion compensation. After image registration, coefficients of correlation between the static image and the motion-corrected and non–motion-corrected images were computed. Total activity in the reconstructed static and motion-corrected images was determined by summing the activities in all phantom slices.

^{99m}Tc-MDP Bone Imaging

A ^{99m}Tc-MDP bone imaging study was performed to test the capability of the system to image a biologic structure in which there is an obvious correlation with anatomy. The capacity for motion correction can be easily assessed as a follow-up to phantom studies. ^{99m}Tc-MDP SPECT images are comparable in appearance to low-resolution CT scans of the skeleton. All procedures were performed in accordance with a protocol approved by the Johns Hopkins University Animal Care and Use Committee.

BALB/c mice (*n* = 3, 30 g) were anesthetized for 10 min with 1.5%–2.0% isoflurane inhalant first by placement in an induction chamber and then with a nose cone while 3 retroreflective fiducial markers were glued to the head in a triangular pattern. A marker was placed on the forehead adjacent to each ear, and the third marker was placed on the nasal bridge. Typically, 30 min later, 122.1 MBq (3.3 mCi) of ^{99m}Tc-MDP was injected through the tail vein. Imaging of the awake mouse began 81 min after injection.

Mice typically were fully awake approximately 20 min after anesthesia was removed, and the scans were initiated at least 30 min after injection to provide sufficient time for the uptake of ^{99m}Tc-MDP. SPECT scanning parameters were 20 s per γ-camera position for 60 increments over 360°. The energy window was 125–155 keV. The optical tracking rate was 10 frames/s for each camera. After imaging in the awake state, the mouse was euthanized,
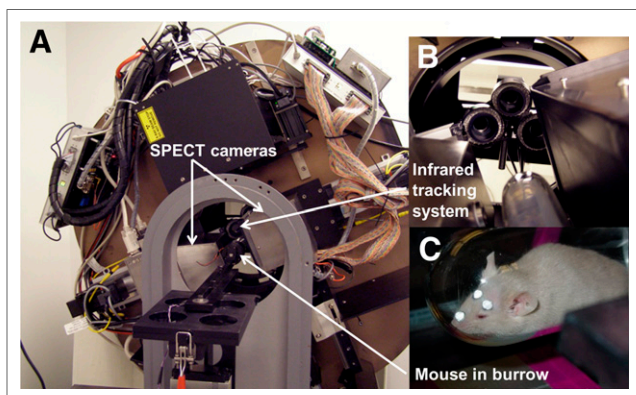

FIGURE 1. AwakeSPECT system. (A) Gantry with SPECT cameras, pinhole collimators, and NIR tracking system. (B) Close-up of NIR tracking system. (C) Mouse in burrow with retroreflective markers affixed to its head.

and a repeat SPECT scan was obtained with the aforementioned parameters. Finally, a micro-CT scan was obtained with the CT scanner on the AwakeSPECT system. Cross-correlations between the motion-corrected and non–motion-corrected scans that were registered to the static scan were computed. Only the skull region was included when the correlations were computed.

123I-Ioflupane Brain Imaging

The binding potential of ^{123}I-ioflupane was assessed in BALB/c mice imaged with ($n = 7$) and without ($n = 4$) anesthesia. The average mouse mass was 37.3 ± 6.6 g (mean $\pm$ SD). Mice that underwent anesthesia were anesthetized as described earlier with 1.5%–2.0% isoflurane inhalant first in the induction chamber and then with a nose cone while fiducial markers were affixed to the head. Mice imaged in the awake state did not undergo anesthesia at any time. Mice were injected with 165.7 ± 8.0 MBq (4.48 ± 0.22 mCi) of ^{123}I-ioflupane through the tail vein. For each mouse, two 25-min scans were acquired beginning 15 (SD, 1.44) and 45 (SD, 1.64) min after injection. The energy window was 142–176 keV. After euthanasia, CT scans were acquired at 300 ms/projection for 360 projections over 360° at 70 kVp with a 500-μA anode current. SPECT image reconstruction parameters were the same as those for the ^{99m}Tc-MDP study. SPECT images were reconstructed with motion compensation. Regions of interest were drawn in the left and right striata and the cerebellum, and the mean radioactivities in the regions of interest were computed. The radiotracer binding potential was calculated as (STR/CER − 1), where STR was the radioactivity in the striata and CER was that in the cerebellum.

Corticosterone Measurements

Plasma corticosterone levels have been used as a surrogate for the degree of stress experienced by animals undergoing experimental procedures (14,15). Corticosterone levels were measured in 3 adult female CD-1 mice that averaged 37.0 g and that underwent a mock AwakeSPECT study. These mice underwent the same preparation as mice used for SPECT brain imaging in the awake state but were injected with an identical volume of sterile saline solution rather than radiotracer. They were then placed in the AwakeSPECT scanner for a mock scan with identical acquisition parameters. Blood was withdrawn from the tail vein after saline injection to provide a baseline value and immediately after the mock scan, which was completed 1 h after injection. Blood was stored in heparin-filled microcontainers (BD) at −80°C until assay. Blood samples were thawed immediately before assay and spun at 1,000g, and the plasma was separated. Corticosterone levels in spun plasma were determined with the Corticosterone EIA Kit ADI-900–097 (Enzo Life Sciences) in accordance with the manufacturer's instructions. All plasma samples were diluted to 500 μL with Assay Buffer 15 (in accordance with kit instructions), and 100 μL of diluted plasma from each set of mouse samples was collected before and after the mock SPECT scans were analyzed. These samples were assayed in triplicate along with standards provided by the manufacturer. The mice were always fully conscious and only briefly restrained with a cylindric mouse restrainer for the administration of saline through the tail vein as well as for tail vein blood withdrawal.

Statistical Analyses

Data are presented as mean $\pm$ SD. Changes in the binding potential were subjected to a 2-tailed Mann–Whitney test with SPSS Statistics 20 software (IBM). A probability level of less than 0.05 was considered significant.

RESULTS

Phantom Imaging

Figure 2 shows slices through reconstructed images of the static scan and moving scans with and without motion correction. All slices were 0.5 mm thick, which was the voxel dimension used during image reconstruction. Image slices through the hot rods of the Ultra-Micro Phantom are shown in the middle row of Figure 2; the same color scale was used for all images. The hot rods for the 4 largest sectors (diameters of 1.35–2.4 mm) could easily be visualized for the static scan and moving scan with motion correction, and the image quality was comparable. For the moving scan without motion correction, the image quality was inferior, and the largest (2.4-mm-diameter) rod could barely be visualized. The peak intensity of the rods on the images without motion correction was lower because activity was blurred into adjacent voxels. For the entire phantom, the coefficients of correlation of the static image with the motion-corrected image and with the non–motion-corrected image were 0.972 and 0.904, respectively. When only the hot-rod slices were used, the coefficients of correlation with the motion-corrected image and with the non–motion-corrected image were 0.947 and 0.859, respectively.

Slices in the central axial plane for the Defrise phantom also are shown in Figure 2. Alternating hot and cold disks could easily be visualized on the static and motion-corrected images, whereas blurring was evident on the non–motion-corrected image. The coefficients of correlation of the static image (computed from all slices) with the motion-corrected image and with the non–motion-corrected image were 0.960 and 0.817, respectively. For
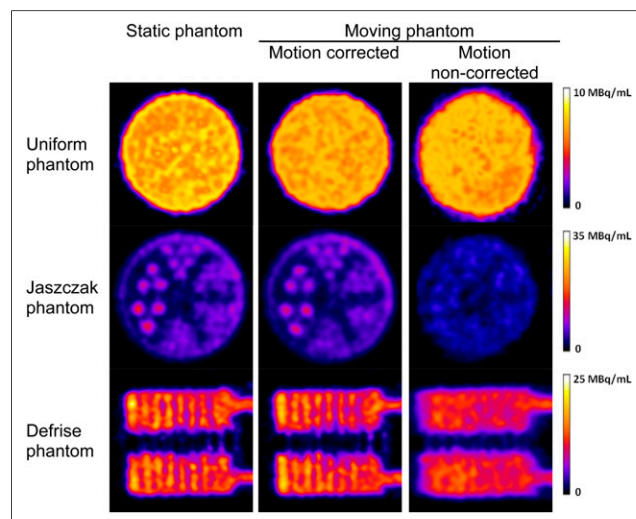

FIGURE 2. Reconstructed image slices through cylindric Ultra-Micro Phantoms that contained no insert (uniform) (top row), hot-rod insert (middle row), and Defrise insert of alternating hot and cold disks (bottom row). Hot-rod diameters were 0.75, 1.0, 1.35, 1.7, 2.0, and 2.4 mm; disk diameter and spacing were 1.62 mm. Motion-corrected images were similar to static phantom images, whereas non–motion-corrected images showed blurring and motion artifacts.

the uniform phantom image without motion correction (top row of Fig. 2), the transaxial slices were distorted from their true circular shape. Angular sampling of activity at a given location in an object or animal is not as uniform in the presence of motion as it is in the static condition, and there is further variability in the spatially dependent point spread function for pinhole imaging. This situation may cause a non-isotropic response in a reconstructed image, resulting in slight elliptic distortions in cross-sections through hot rods.

Total activities for the Ultra-Micro Jaszczak, Defrise, and uniform phantoms with motion correction were 95.5%, 94.9%, and 95.9%, respectively, of the total activities measured for the static scan. Potential reasons for the differences include a lack of modeling of photon penetration and scattering near the pinhole aperture that varies as a function of source position.

^{99m}Tc-MDP Bone Imaging

The mouse was alert, with moderate head motion, throughout the scan (Fig. 3). Total scan time was 1,380 s, and data acquisition time was 1,224 s; the discrepancy was the result of data dropouts (see explanation later in paragraph). The head pose is defined as the 3 translational and 3 rotational degrees of freedom describing the head position and orientation. There was an extremely low net loss of data attributable to the loss of pose tracking (i.e., 460/7,948 = 5.8%). There was a low percentage of usable (but not used for the reconstruction presented here) data collected during gantry motion steps (i.e., 1,013/8,961 = 11.3%). The percentage of collected data used during motion-corrected image reconstruction was 83.6% (i.e., 7,488/8,961). The number of pose bins was indicative of the degree of animal motion or activity during scanning in the awake state.

The optical tracking system was able to provide pose measurements for more than 94% of all acquired image positions. Poses that were not acquired successfully were primarily attributable to the mouse turning away from the cameras, with the head oriented up. Dropped data generally were the result of mouse head motion away from the cameras, so that the markers were not visible on the images. In some cases, measurement errors or spurious reflections may result in a model fit with errors outside the normal bounds. No measurement is reported when this happens. The total number of pose bins was 2,387, and each pose bin contained an average of 192 γ-ray events.

Orthogonal slices through the reconstructed SPECT images are shown in Figure 3. There was excellent agreement between the images from motion-corrected scans of awake animals and the images from postmortem SPECT scans. These showed structures for the skull and jaw similar to those shown on CT scans, although at a lower resolution. There were obvious blurring artifacts in non–motion-corrected scans of awake animals.

For mouse 1, the coefficients of correlation of the static image of the skull region with the motion-corrected image and with the non–motion-corrected image were 0.935 and 0.736, respectively. For mouse 2, the respective correlations
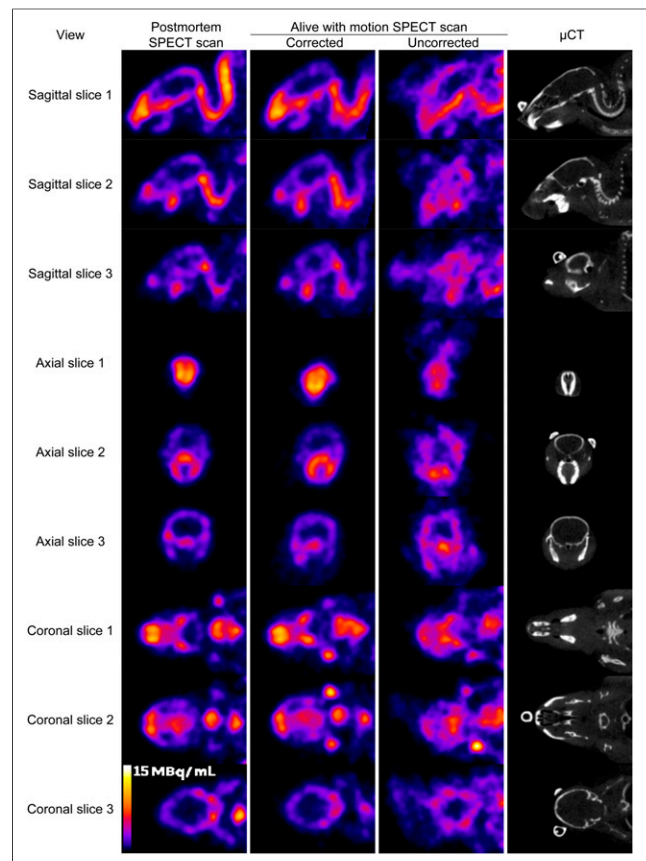

FIGURE 3. Matched reconstructed image slices for ^{99m}Tc-MDP mouse scans. Each row shows slices for postmortem scan (column 1), awake scan with motion correction (column 2), awake scan without motion correction (column 3), and postmortem small-animal CT scan (μCT) (column 4). Three different slices were provided for each set of sagittal, transaxial, and coronal images. Images from awake scans with motion correction provided detail similar to that provided by static postmortem scans, whereas images from awake scans without motion correction showed blurred and misshapen features. Attached retroreflectors could be seen on several small-animal CT slices.

were 0.926 and 0.682. The higher correlations obtained with motion correction were in accord with qualitative observations from the reconstructed images. The difference in the values obtained without motion correction reflected, in part, a difference in the amounts of head motion between the 2 animals; mouse 2 had greater head motion. For mouse 1, the SDs of the pose measurements were 1.3, 0.8, and 1.3 mm for the translational degrees of freedom and 12.1°, 13.5°, and 38.2° for the 3 rotational degrees of freedom. For mouse 2, the corresponding SDs were 2.2, 1.7, and 1.3 mm for the translational degrees of freedom and 36.2°, 19.6°, and 54.3° for the 3 rotational degrees of freedom. The correlations of the static scan with the motion-corrected scan were not expected to be perfect because of image noise and the fact that the scan of an awake animal represented an average of the radiotracer biodistributions during the scan whereas the postmortem static scan represented the end-state biodistribution. AwakeSPECT provided SPECT

bone images that were similar in appearance to images obtained from small-animal CT imaging but had lower spatial resolution.

[123]I-Ioflupane Brain Imaging

Head motion was tracked 90%–95% of the time for the scans of awake animals. Representative image reconstructions for anesthetized and awake mice are shown in Figure 4 for the scan from 15 to 40 min fused with a coregistered CT image. The radiotracer uptake pattern in the scans of awake animals was strikingly different from that in the scans acquired under anesthesia, and striatal uptake was higher in the anesthetized mice. For the first scan (15–40 min after injection), the striatal binding potential in the awake mice averaged 33% of that in the mice scanned under anesthesia. For the second scan (45–70 min after injection), the awake mice had an average binding potential that was 50% that in the anesthetized mice. Table 1 shows the ratio of the binding potential in the awake mice ($n = 4$) to that in the anesthetized mice ($n = 7$). Differences between the awake and anesthetized states were significant in both striata for scan 1 and in the left striatum for scan 2.

Corticosterone Measurements

Corticosterone levels are reported in mean $\pm$ SD nanograms of corticosterone per milliliter (Table 2). Two mice handled and prepared for AwakeSPECT scans experienced 1.8–2.7 times higher corticosterone levels after imaging

FIGURE 4. Image reconstruction results for ^{123}I-ioflupane SPECT scans of anesthetized mouse (left) and awake mouse (right) coregistered with CT. Higher striatal uptake was observed in anesthetized mouse. Image scale peak of 48 MBq/mL corresponded to approximately 29% of injected dose/mL. Right striatum was identified on transaxial images (yellow broken circle).

than at baseline. This increase was consistent with that observed in mice exposed to behavioral stimuli such as olfactory stimulation with rat odors (23), in which corticosterone levels showed an average increase of 1.75-fold after exposure, as well as with prior imaging studies of awake animals (14,15), in which corticosterone levels showed average increases of approximately 4- to 5-fold by 1 h after injection. We observed that the weight of each mouse influenced its propensity for movement and agitation within the scanning burrow. Mice weighing less than 35 g tended to appear more comfortable and moved less than mice weighing 40 g or more; the snug fit for the latter resulted in increased agitation. NIR-transparent scanning burrows can be matched to the sizes of animals to minimize anxiety during scanning.

DISCUSSION

AwakeSPECT is the first system developed for SPECT imaging of conscious, unrestrained small animals. It uses NIR cameras to track the position of the head of an awake mouse or moving source object during SPECT imaging and then uses this tracking information to correct for motion during SPECT image reconstruction. The construction and specifications of the AwakeSPECT system were described previously (Fig. 1) (18,21). Although we obtained static scans in this series of studies, the AwakeSPECT system is equally applicable to dynamic imaging.

This is the first report to describe the ability of AwakeSPECT to correct for motion in a study of conscious animals. Visual inspection of the phantom and live-animal imaging studies with ^{99m}Tc-MDP and ^{123}I-ioflupane indicated that AwakeSPECT images are comparable to images of animals scanned under anesthesia (Figs. 2–4).

The first live-animal study involved bone scanning, which is often performed as a proof-of-principle study in the construction of small-animal molecular imaging devices, because the bony detail simulates that found in a microphantom and is easily appreciated on CT (24). However, small-animal molecular bone imaging has also proved to be an important way to evaluate metastases in experimental models of cancer, in correlation with anatomic imaging studies, that is, radiography and CT (22,25). The second live-animal study, with ^{123}I-ioflupane, provided a more relevant example of the utility of AwakeSPECT, proving that it can be used for motion correction in a brain-targeted experimental radiotracer imaging study.

To provide an understanding of pharmacokinetics, identify target substructures, and develop quantitative models, central nervous system radiopharmaceutical development frequently involves imaging in nonhuman primates before clinical studies. However, with exceptions beginning to emerge (26,27), such studies involve animals under general anesthesia. Anesthesia is well known to cause substantial fluctuations in radiotracer uptake through alterations in delivery (cerebral blood flow) and brain metabolism,
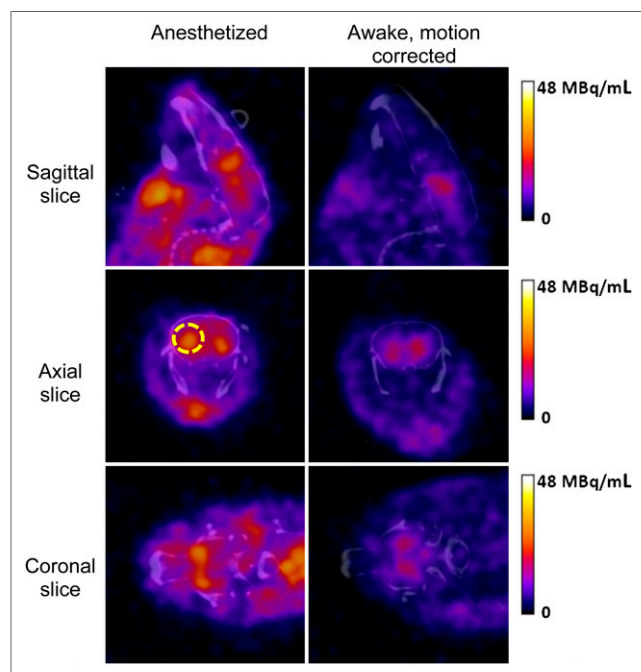
TABLE 1
Binding Potential Results for ^{123}I-Ioflupane Imaging

| Scan | Binding potential (mean ± SD) in: | | R (%) | Mean R (%) |
	Anesthetized mice	Awake mice		
1 (15–40 min)				32.8
Left	2.43 ± 1.02	0.68 ± 0.29	28.0	
Right	2.21 ± 1.07	0.83 ± 0.53	37.6	
2 (45–70 min)				49.6
Left	2.12 ± 0.41	0.97 ± 0.18	45.8	
Right	2.00 ± 0.60	1.07 ± 0.29	53.5	

R = ratio of binding potential in awake mice to that in anesthetized mice.

suggesting that studies performed under anesthesia are only rough guides for the clinical studies to follow (*23,28*). Nonhuman primate studies are expensive, laborious, and not amenable to large sample sizes. Although possible and often done, obtaining histopathologic correlations from nonhuman primate studies is difficult. Mice can be manipulated genetically, enabling testing of new radiotracers in relevant transgenic mice to determine target specificity. For these reasons, as well as the ability to monitor experimental models longitudinally, AwakeSPECT can augment preclinical studies of SPECT radiotracers.

Dopaminergic transmission has been linked to various aspects of behavior, such as movement, motivation, and cognition (*29*). Originating within the substantia nigra of the midbrain, dopaminergic neurons largely innervate the striatum, which has become a proving ground for investigating the effects of anesthesia as well as other aspects of neurotransmission in preclinical imaging studies. Our determination that the binding potential of ^{123}I-ioflupane in the awake state was 33%–50% that in anesthetized animals is in keeping with the lower dopamine transporter radioligand uptake observed in a nonhuman primate study (*30*). The explanation provided in that study was that isoflurane enhanced the production of nitric oxide, which in turn facilitated the uptake of dopamine transporter radioligands. The data suggested that indirect mechanisms may contribute to confounding of results by anesthesia. In fact, the effects of anesthesia on cerebral blood flow alone are species and strain dependent, differ by brain region, and vary—often in opposite directions—by anesthetic. Such findings underscore further the importance of imaging in the awake state, which best mimics the most relevant human condition.

Three other devices were recently developed for imaging small animals in the awake state. The RatCAP was developed by the Brookhaven Group to couple animal molecular neuroimaging with behavioral studies (*15*). The RatCAP is a miniature PET scanner that is surgically attached to the rat skull with a counterweight, enabling reasonably free movement of the animal. Although this device requires substantial training and acclimation of the animal, information about the pharmacokinetics of ^{11}C-raclopride (which binds primarily to postsynaptic D_2-dopamine receptors) was obtained in awake, active rats; the device provided results that may further inform the understanding of dopaminergic transmission. The solution of Mizuma et al. to the imaging of awake animals involved head immobilization—surgically implanting an acrylic head fixture that was then attached to a holder within a commercial PET system (*14*). They were able to quantify the regional rate of glucose metabolism in the mouse brain with full kinetic modeling focusing on the effects of various manipulations, such as warming, catheterization, and acclimation, on glucose uptake. Consistent with earlier studies in nonhuman primates and humans, they found an elevated regional rate of glucose metabolism in the conscious state relative to the anesthetized state. Fulton et al. (*31*) are developing a system for PET imaging of awake mice and rats that does not require prior surgery. Their approach uses a robot-driven animal motion compensation system. The animals are free to move in a chamber placed inside the PET scanner. The position of an animal is tracked through an optical tracking system, and the motion information is used in real time to direct a robot arm to keep the animal in the same orientation and location in the PET scanner. Animal imaging studies have not yet been reported for this system.

An important aspect of the 2 earlier PET studies of awake animals as well as our SPECT study is the degree of stress to which the animals were subjected before and during the imaging session. A surrogate measure of such

TABLE 2
Serum Corticosterone Levels in Mice Before and After Mock AwakeSPECT Scan

| Mouse | Corticosterone (mean ± SD pg/mL) | | Postscan-to prescan ratio |
	Prescan	Postscan	
1	19.93 ± 0.04	52.81 ± 0.06	2.65
2	8.48 ± 0.04	82.77 ± 0.15	9.76
3	7.72 ± 0.03	14.37 ± 0.03	1.86

stress is the level of serum corticosterone, a stress hormone in rodents, with higher levels indicating greater stress. In the RatCAP study (15), corticosterone levels were measured before attachment of the scanner and at several time points thereafter. Corticosterone levels in the 2 rats studied increased approximately 4-fold from baseline levels at 10 min after attachment, nearly normalized in 1 rat at 3 h, and decreased only to about twice the baseline levels in the other rat at this time. In the other PET study (14), on the first day after surgery to affix the head holder to the animal, corticosterone levels were elevated 4-fold from baseline levels and remained elevated at least 2-fold 30 d after surgery. Similarly, we found an approximately 3-fold increase in serum corticosterone levels after scanning (compared with before scanning), which occurred 1 h after placement of the mice in the burrow. Unlike the investigators in those 2 studies, however, we did not train or otherwise acclimate the mice to the procedure. Although the reflective markers attached to the heads of the mice to track motion could certainly have caused some stress, no surgery was involved. A modest amount of movement was permitted in the burrow, but behavioral studies like those performed with the RatCAP would not be possible with our system. Because of the lack of surgery or training, the AwakeSPECT system is essentially ready to use on any mouse and is likely more amenable to repeat studies than the other systems.

Motion tracking measurements are obtained from images taken near the front of the burrow through the hemispherical glass head, suggesting the possibility of the introduction of an error attributable to refraction. The glass burrow wall is about 2 mm thick. Three reflective markers spaced 20–30 mm apart are tracked to calculate a 3-dimensional pose. Refraction errors, as discussed by Kyme et al. (32), were considered negligible in the present study. Such errors (<0.03 mm) were much smaller than the overall root-mean-square tracking accuracy of 0.2 mm for our system.

CONCLUSION

The AwakeSPECT system conveniently enables imaging of conscious mice in the absence of physical or chemical restraint and does not require prior training or significant acclimatization of animals before the scanning session. Motion correction enables quantification of the binding potential of the dopamine transporter radioligand ^{123}I-ioflupane, which is used clinically in the assessment of neurodegenerative and movement disorders (19,20). Such studies can be generalized to encompass a wide variety of transgenic and other relevant animal models of human disease. Additional detector heads can be added to improve sensitivity, and the burrow can be modified to study larger animals, such as rats.

DISCLOSURE

ACKNOWLEDGMENTS

REFERENCES

1. Hillman EM. Optical brain imaging in vivo: techniques and applications from animal to man. *J Biomed Opt.* 2007;12:051402.
2. Fomchenko EI, Holland EC. Mouse models of brain tumors and their applications in preclinical trials. *Clin Cancer Res.* 2006;12:5288–5297.
3. Weissleder R. Scaling down imaging: molecular mapping of cancer in mice. *Nat Rev Cancer.* 2002;2:11–18.
4. Lewis JS, Achilefu S, Garbow JR, Laforest R, Welch MJ. Small animal imaging: current technology and perspectives for oncological imaging. *Eur J Cancer.* 2002;38:2173–2188.
5. Piyawattanametha W, Cocker ED, Burns LD, et al. In vivo brain imaging using a portable 2.9 g two-photon microscope based on a microelectromechanical systems scanning mirror. *Opt Lett.* 2009;34:2309–2311.
6. Barretto RP, Ko TH, Jung JC, et al. Time-lapse imaging of disease progression in deep brain areas using fluorescence microendoscopy. *Nat Med.* 2011;17:223–228.
7. Roe AW. Long-term optical imaging of intrinsic signals in anesthetized and awake monkeys. *Appl Opt.* 2007;46:1872–1880.
8. Lahti KM, Ferris CF, Li F, Sotak CH, King JA. Imaging brain activity in conscious animals using functional MR imaging. *J Neurosci Methods.* 1998;82:75–83.
9. Shtoyerman E, Arieli A, Slovin H, Vanzetta I, Grinvald A. Long-term optical imaging and spectroscopy reveal mechanisms underlying the intrinsic signal and stability of cortical maps in V1 of behaving monkeys. *J Neurosci.* 2000;20:8111–8121.
10. Shimoji K, Ravasi L, Schmidt K, et al. Measurement of cerebral glucose metabolic rates in the anesthetized rat by dynamic scanning with ^{18}F-FDG, the ATLAS small-animal PET scanner, and arterial blood sampling. *J Nucl Med.* 2004;45:665–672.
11. Martin C, Martindale J, Berwick J, Mayhew J. Investigating neural-hemodynamic coupling and the hemodynamic response function in the awake rat. *Neuroimage.* 2006;32:33–48.
12. Tassonyi E, Charpantier E, Muller D, Dumont L, Bertrand D. The role of nicotinic acetylcholine receptors in the mechanisms of anesthesia. *Brain Res Bull.* 2002;57:133–150.
13. Dombeck DA, Khabbaz AN, Collman F, Adelman TL, Tank DW. Imaging large-scale neural activity with cellular resolution in awake, mobile mice. *Neuron.* 2007;56:43–57.
14. Mizuma H, Shukuri M, Hayashi T, Watanabe Y, Onoe H. Establishment of in vivo brain imaging method in conscious mice. *J Nucl Med.* 2010;51:1068–1075.
15. Schulz D, Southekal S, Junnarkar SS, et al. Simultaneous assessment of rodent behavior and neurochemistry using a miniature positron emission tomograph. *Nat Methods.* 2011;8:347–352.

16. Hildebrandt IJ, Su H, Weber WA. Anesthesia and other considerations for in vivo imaging of small animals. *ILAR J.* 2008;49:17–26.

17. Wang J, Rao H, Wetmore GS, et al. Perfusion functional MR imaging reveals cerebral blood flow pattern under psychological stress. *Proc Natl Acad Sci USA.* 2005;102:17804–17809.

18. Weisenberger AG, Lee S, Smith MF. Motion-tracking technique in unrestrained small-animal single-photon emission computed tomography. *Rev Neurosci.* 2011;22:657–663.

19. Catafau AM, Tolosa E. Impact of dopamine transporter SPECT using ^{123}I-ioflupane on diagnosis and management of patients with clinically uncertain parkinsonian syndromes. *Mov Disord.* 2004;19:1175–1182.

20. McKeith I, O'Brien J, Walker Z, et al. Sensitivity and specificity of dopamine transporter imaging with ^{123}I-FP-CIT SPECT in dementia with Lewy bodies: a phase III, multicentre study. *Lancet Neurol.* 2007;6:305–313.

21. Goddard JS, Baba JS, Lee SJ, et al. Real-time awake animal motion tracking system for SPECT imaging. *IEEE Nucl Sci Symp Conf Rec.* 2008:4707–4710.

22. Baiker M, Snoeks TJ, Kaijzel EL, et al. Automated bone volume and thickness measurements in small animal whole-body MicroCT data. *Mol Imaging Biol.* 2012;14:420–430.

23. Kaisti KK, Metsahonkala L, Teras M, et al. Effects of surgical levels of propofol and sevoflurane anesthesia on cerebral blood flow in healthy subjects studied with positron emission tomography. *Anesthesiology.* 2002;96:1358–1370.

24. Wang Y, Seidel J, Tsui BM, Vaquero JJ, Pomper MG. Performance evaluation of the GE Healthcare eXplore VISTA dual-ring small-animal PET scanner. *J Nucl Med.* 2006;47:1891–1900.

25. Johnson LC, Johnson RW, Munoz SA, Mundy GR, Peterson TE, Sterling JA. Longitudinal live animal micro-CT allows for quantitative analysis of tumor-induced bone destruction. *Bone.* 2011;48:141–151.

26. Katsuyama N, Imamura K, Onoe H, et al. Cortical activation during color discrimination task in macaques as revealed by positron emission tomography. *Neurosci Lett.* 2010;484:168–173.

27. Schoultz BW, Hjornevik T, Willoch F, et al. Evaluation of the kappa-opioid receptor-selective tracer [^{11}C]GR103545 in awake rhesus macaques. *Eur J Nucl Med Mol Imaging.* 2010;37:1174–1180.

28. Laitio RM, Langsjo JW, Aalto S, et al. The effects of xenon anesthesia on the relationship between cerebral glucose metabolism and blood flow in healthy subjects: a positron emission tomography study. *Anesth Analg.* 2009;108:593–600.

29. Rice ME, Patel JC, Cragg SJ. Dopamine release in the basal ganglia. *Neuroscience.* 2011;198:112–137.

30. Tsukada H, Nishiyama S, Kakiuchi T, et al. Isoflurane anesthesia enhances the inhibitory effects of cocaine and GBR12909 on dopamine transporter: PET studies in combination with microdialysis in the monkey brain. *Brain Res.* 1999;849:85–96.

31. Fulton RR, Meikle SR, Kyme A, et al. Imaging the awake rat brain with microPET, head tracking and motion correction. In: 5th International Conference on Imaging Technologies in Biomedical Science; September 13–19, 2009, Milos Island, Greece.

32. Kyme A, Meikle SR, Baldock C, Fulton RR. Refraction-compensated motion tracking of unrestrained animals in PET. *IEEE Nucl Sci Symp Conf Rec.* 2010: 3221–3224.